CHINESE OPTICS LETTERS

Vol. 20, No. 3 | March 2022

High performances of diode-end-pumped Nd:$SrAl_{12}O_{19}$ lasers operated in continuous-wave and passively *Q*-switched regimes

Jun Guo (郭 俊)[1], Jian Liu (刘 坚)[2], Jie Xu (徐 杰)[1], Bin Xu (徐 斌)[3], Yuchong Ding (丁雨憧)[4*], Xiaodan Wang (王晓丹)[5], Xiaodong Xu (徐晓东)[1**], and Jun Xu (徐 军)[2]

[1] Jiangsu Key Laboratory of Advanced Laser Materials and Devices, School of Physics and Electronic Engineering, Jiangsu Normal University, Xuzhou 221116, China

[2] School of Physics Science and Engineering, Institute for Advanced Study, Tongji University, Shanghai 200092, China

[3] Department of Electronic Engineering, Xiamen University, Xiamen 361005, China

[4] Research & Development Center of Material and Equipment, 26th Research Institute, China Electronics Technology Group Corporation, Chongqing 400060, China

[5] School of Physics Science and Technology, Suzhou University of Science and Technology, Suzhou 215009, China

*Corresponding author: dingyc@cetccq.com.cn

**Corresponding author: xdxu79@jsnu.edu.cn

Received November 3, 2021 | Accepted December 2, 2021 | Posted Online December 23, 2021

A good thermo-optic property of strontium dodeca-aluminum oxide ($SrAl_{12}O_{12}$, SRA) host material is very advantageous to the development of high-performance lasers by doping rare-earth ions for gain medium. In this work, we report on diode-end-pumped high-performance continuous-wave and passively *Q*-switched Nd:SRA lasers. For continuous-wave operation, a maximum output power of 6.45 W is achieved at 1049 nm with a slope efficiency of about 41.6%. Using a $Y_3Al_5O_{12}$ (YAG) etalon, we have firstly achieved a 1066 nm laser with a maximum output power of 4.15 W and a slope efficiency of about 27%, to the best of our knowledge. For passively *Q*-switched operation, with Cr^{4+} : YAG as a saturable absorber, a maximum average output power of 1.82 W was achieved with the shortest pulse width of 18.2 ns at pulse repetition rate of 22.9 kHz. The single-pulse energy and pulse peak power were 79.4 μJ and 4.3 kW. This work has further verified that the Nd:SRA crystal is very promising for high-performance laser generation.

Keywords: diode pump; Nd:SRA crystal; continuous-wave operation; passively *Q*-switched operation.
DOI: 10.3788/COL202220.031401

1. Introduction

During past years, disordered laser material with a broadened emission spectrum has attracted great attention because of its advantages in achieving laser sources with tunable lasing wavelengths. For example, in early 2004, Rico *et al.* reported a wavelength tunable operation in a disordered Yb:$NaGd(WO_4)_2$ laser[1]. In 2009, Yu *et al.* reported a dual-wavelength operation in a disordered Nd:$Ca_3Nb_{1.5}G_{3.5}O_{12}$ (Nd:CNGG) laser[2]. Nd:$La_3Ga_5SiO_{14}$, one of the oxyorthosilicate materials, has been demonstrated to tunably lase at about 900 nm[3]. Another disordered oxyorthosilicate material, Nd:$LuYSiO_5$ crystal, was also reported to have many lasing possibilities at various emission lines[4]. Disordered laser material has another very important advantage, namely generating a femtosecond ultrashort pulse laser. For instance, in 2009, Xie *et al.* demonstrated a 900 fs laser using a Nd:$Ca_3Li_{0.275}Nb_{1.775}Ga_{2.95}O_{12}$ (Nd:CLNGG) disordered crystal[5]. In 2014, Qin *et al.* reported a mode-locked disordered Nd,Y:CaF_2 laser with a pulse time duration down to 103 fs[6]. In 2016, Ma *et al.* achieved a mode-locked Nd:$Ca_3La_2(BO_3)_4$ disordered laser with a pulse width as short as 79 fs[7].

Strontium dodeca-aluminum oxide, $SrAl_{12}O_{19}$ (SRA), has the magneto-plumbite structure and the space group $P6_3/mmc$ [8]. As one of the efficient Pr^{3+}-doped oxides, this host material gains its success in Pr^{3+} visible lasers[9–11]. In fact, SRA has been reported to have advantages of high thermal conductivity of 11 $W{\cdot}m^{-1}{\cdot}K^{-1}$ for 1% (atomic fraction) Pr,Mg:SRA and large Moh's hardness of nine[9,10]. It is well-known that the two merits are very crucial for power scaling. Besides being doped with Pr^{3+}, the SRA host has also been recently demonstrated

© 2022 Chinese Optics Letters

to lase in Nd^{3+}:SRA crystals[12,13]. However, on the one hand, the reported lasing wavelength has only been limited at 1049 nm corresponding to the highest gain peak. On the other hand, the laser performances [31.3% of slope efficiency for continuous-wave (CW) operation[13]; peak power and single-pulse energy of 1.87 W and 0.65 μJ for passively *Q*-switched operation[12]] in the two works left room for performance enhancements.

In this work, firstly, we have made efforts to realize laser operation at wavelengths different from the typical 1049 nm line. Using an etalon as wavelength selector, we have achieved lasing behavior at 1066 nm in a diode-pumped Nd:SRA laser. Moreover, dual-wavelength operation at 1049 and 1066 nm was also readily obtained, which could have potential applications in medical instrumentation, spectral analysis, optical frequency up-conversion, terahertz (THz) frequency generation, etc. Secondly, we have greatly improved laser performances of the CW and passively *Q*-switched Nd:SRA lasers.

2. Experimental Details

The laser experimental setup is shown in Fig. 1 schematically. A fiber-coupled 793 nm diode laser having a maximum output power of 30 W was used as the pump source with core diameter of 105 μm and numerical aperture of 0.22. The pump beam was injected into the laser crystal through a collimated lens with a focal length of 40 mm and a focusing lens with a focal length of 75 mm, which leads to a pump beam waist size of about 200 μm. The laser resonator was arranged into a simple two-mirror configuration. The input mirror (M1) is a concave mirror with curvature radius of 100 mm, and the M1 mirror has a high transmission coating of 94% at the pumping wavelength and high reflection of 99.9% at lasing wavelengths. In order to explore the laser performance sufficiently, in the experiment, five flat mirrors (M2) were used as output couplers (OCs), respectively, with transmissions of about 1.9%, 4.7%, 6.2%, 8.9%, and 12.1%.

The laser gain medium is an *a*-cut Nd:SRA crystal with dimensions of 3 mm × 3 mm × 6 mm and dopant concentration of 5% (atomic fraction). The Nd:SRA crystal was grown by the Czochralski method from an inductively heated iridium crucible. Nd^{3+} ions occupy the divalent Sr site in SRA. Therefore, the same concentration of Mg^{2+} co-doped on the Al site is required as a charge compensation. The single-pass absorption ratio of the pump power was estimated to be about 58.1% at maximum pump power by measuring the incident pump power and transmitted pump power, and, at the same time, estimating the reflected power. We wrapped the laser crystal with indium foil and then mounted it inside a copper block that was connected with a water-cooled mini-chiller. To protect this crystal from thermal fracture, we set the temperature of the chiller to be 6°C. Moreover, in the experiment, we used a 0.13-mm-thick undoped $Y_3Al_5O_{12}$ (YAG) thin plate as a Fabry–Perot (F-P) etalon for tuning the lasing wavelength. To operate the laser in the pulsed regime, we used anti-reflection-coated Cr:YAG with an initial transmission of 80% for passive *Q*-switching.

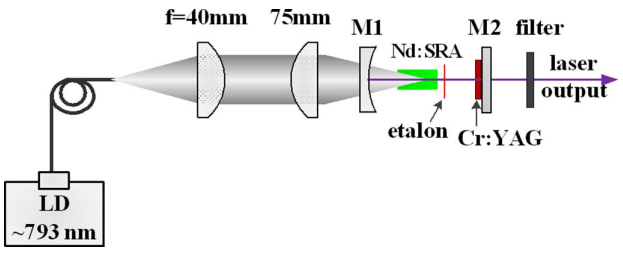

Fig. 1. Laser experimental setup of diode-end-pumped continuous-wave and passively *Q*-switched Nd:SRA lasers.

3. Results and Discussion

The *σ*-polarized emission spectrum of the *a*-cut Nd:SRA crystal from 1000 to 1120 nm is reported in Fig. 2. This emission band corresponds to the $^4F_{3/2} \rightarrow {}^4I_{11/2}$ transition, which exhibits the highest emission intensity with an emission cross section of 3.36×10^{-20} cm^2 at 1048.5 nm. The sub-peak emission line is at 1066.0 nm with an emission cross section of 2.37×10^{-20} cm^2, i.e., about 70% of that of the 1048.5 nm main peak[13]. As we mentioned above, only the 1048.5 nm line has been demonstrated for laser operation at present. However, the comparable and considerable emission cross section of the sub-peak indicates significant lasing potential of this emission line.

Figure 3 reports the output power versus absorbed power of the diode-pumped Nd:SRA lasers under free-running mode, i.e., just the laser gain medium itself and without inserting any other optics inside the resonator. Using the 1.9% low-transmission OC, we achieved a maximum output power of 3.06 W. A slope efficiency of about 18.6% can be deduced by linear fit of the data. For achieving higher output power, it is necessary to use an OC with higher transmission, as we have tried the OCs of 4.7%, 6.2%, and 8.9% transmission. The maximum output powers reached 4.61 W, 5.25 W, and 5.82 W, respectively. The corresponding slope efficiencies increased to 29.1%, 33.3%, and

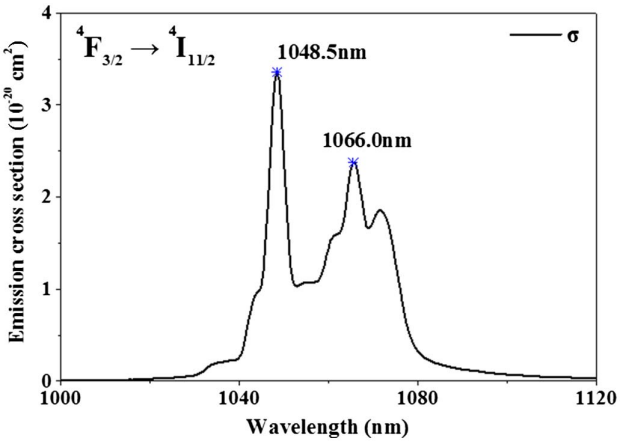

Fig. 2. *σ*-polarized emission spectrum of an *a*-cut Nd:SRA crystal from 1000 to 1120 nm.

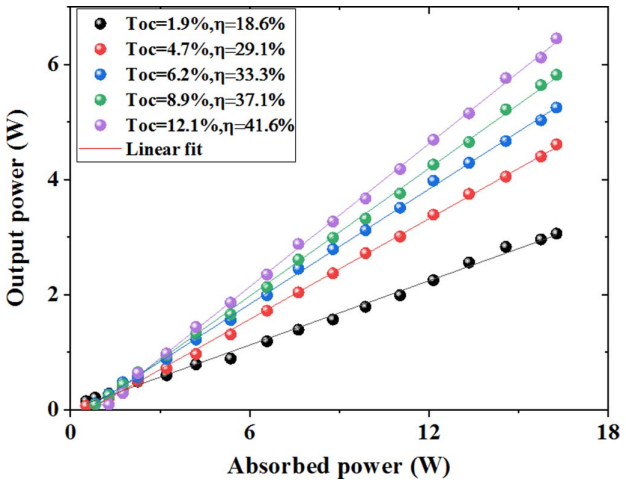

Fig. 3. Output power versus absorbed power of free-running diode-pumped Nd:SRA lasers.

37.1%. In the experiment, the highest output power was obtained to be 6.45 W when the 12.1% transmission OC was employed, which leads to a slope efficiency of about 41.6%. The lasing wavelength is shown in Fig. 4 with an emission peak of 1048.7 nm. Note that, previously, the highest slope efficiency of the diode-pumped Nd:SRA laser at this specific wavelength was reported to be 31.3%[13]. The present efficiency promotion should be attributed to the good mode overlap between the pump beam and cavity mode with an average overlap efficiency of about 89.6% according to the calculation reported in Ref. [14]. Beam quality of the output laser, denoted by the M^2 factor, was measured to be about 3.7 and 3.9 in the x and y directions, as we used during the calculating process. In the past, many Nd lasers have been demonstrated. However, the Nd:YAG laser at 1064 nm has still presented one of the best results. For example, Ref. [15] reported a 15.26 W Nd:YAG laser at 1064 nm with a slope efficiency close to 60%. Nevertheless, on the one hand, comparatively, it is still expected that better laser performance could be achieved in the Nd:SRA laser after further optimization of the total laser system. On the other hand, we would emphasize that the lasing wavelength of 1049 nm cannot be achieved in the Nd:YAG laser, which could potentially be in some specific wavelength-related applications. Moreover, the broadband emission spectrum of the Nd:SRA crystal could indicate femtosecond laser generation via mode-locking technology, which will be our next investigation.

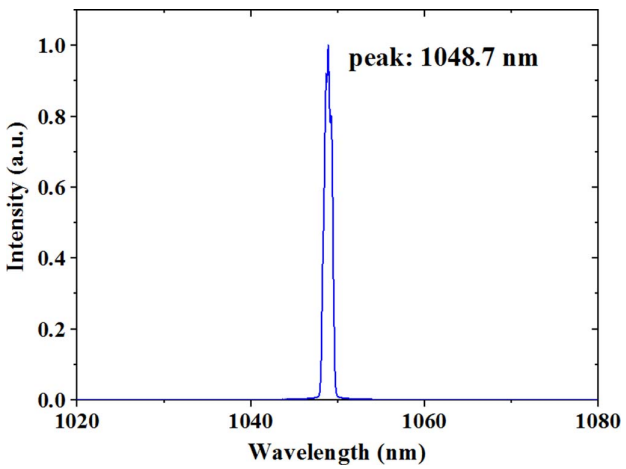

Fig. 4. Laser wavelength of typical Nd:SRA laser under free-running mode.

In this research, we are stimulated to realize laser generation at the sub-peak of 1066 nm, which is reported in Fig. 2 to have considerable emission intensity at this emission line. We therefore inserted an un-doped YAG thin plate as an F-P etalon inside the laser resonator just after the Nd:SRA crystal. By slightly tilting the etalon to a little bit larger than 3°, we found that the 1049 nm lasing with higher emission intensity can be totally suppressed, and a single-wavelength 1066 nm laser can be generated. Under this situation, we can estimate that the etalon introduced an extra loss of about 28% for the 1049 nm line using the transmission expression of the etalon:

$$T = \frac{(1-R)^2}{(1-R)^2 + 4R\sin^2\left(\frac{2\pi n l_e \cos\theta}{\lambda}\right)},$$

where R is the reflectivity for one surface of the etalon, n and l_e are the refractive index and thickness of the etalon, λ is the wavelength, and θ is the incident angle of the cavity mode to the etalon.

Figure 5 shows the output power evolving with the absorbed power. Note that in this experiment we only used the 12.1% transmission OC since we achieved the best result with it, as shown above. The maximum output power reached 4.15 W, and the linearly fitted slope efficiency was about 27.0%. The lasing wavelength is shown in Fig. 6 with a peak at 1066.3 nm. Moreover, we noticed that the 1066 nm laser has a linewidth of 0.99 nm (FWHM value), while it is about 1.09 nm for the 1049 nm laser. We set the same resolution of 0.05 nm for the used optical spectrum analyzer. It should be pointed out that

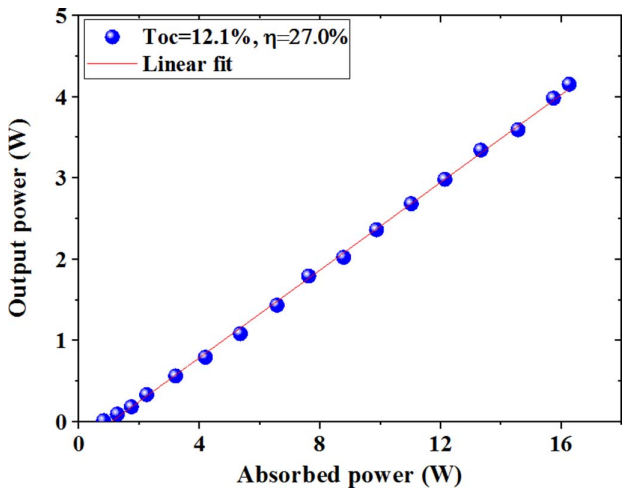

Fig. 5. Output power versus absorbed power of diode-pumped Nd:SRA laser under the insertion of a YAG etalon for wavelength tuning.

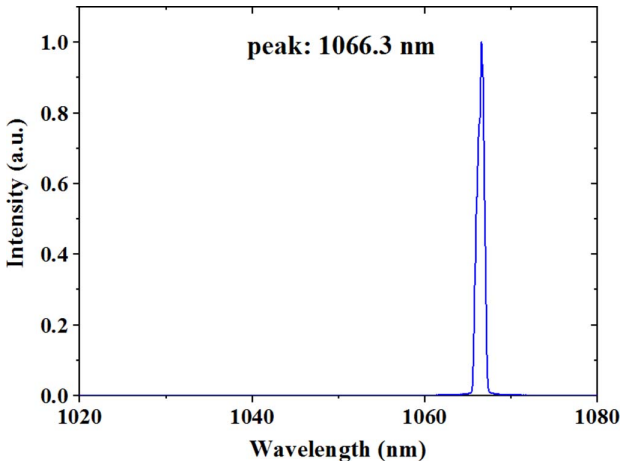

Fig. 6. Typical laser wavelength after the insertion of the YAG etalon.

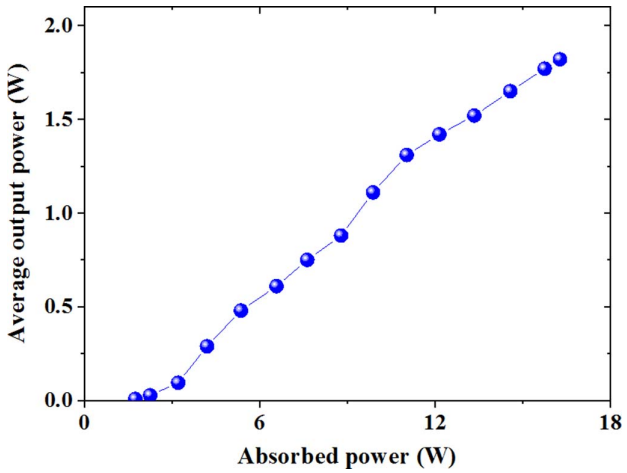

Fig. 8. Average output power versus absorbed power of passively *Q*-switched Nd:SRA laser.

a simultaneous dual-wavelength lasing behavior can also be achieved if we tilted the YAG etalon to a suitable angle. Figure 7 shows the lasing wavelength of the dual-wavelength laser at a total maximum output power of 4.86 W.

The peak wavelengths are 1049.4 nm and 1066.2 nm with comparable intensities by intentionally tilting the etalon since it is really wanted for some applications. One may notice that under the dual-wavelength case the two lasing peaks are different from the case when we achieved them individually. This phenomenon is generally explained by the etalon effect, as the maximum transmission of the etalon is wavelength related.

A passively *Q*-switched Nd:SRA laser has been once reported recently using a MXene $Ti_3C_2T_x$ saturable absorber (SA)[12]. Such nanomaterial SAs are now popular for pulsed laser generation[16–19]. However, due to the low damage threshold and limited modulation depth, it is still very challenging to produce high-performance passively *Q*-switched lasers via nanomaterial SAs. As reported in Ref. [12], the achieved average output power, peak power, and single-pulse energy are only 0.13 W, 1.87 W, and 0.65 μJ. In the following, using a conventional Cr:YAG SA for the passively *Q*-switched laser, we achieved a high average output power as high as 1.82 W at a maximum absorbed power of 16.2 W (see Fig. 8). At the maximum, the pulse trains show a pulse interval of about 43.6 μs for two neighboring pulses, which corresponds to a pulse repetition rate of about 22.9 kHz [see Fig. 9(a)]. Moreover, under this situation, the pulse width is found to be about 18.2 ns, as shown in Fig. 9(b). In addition, pulse-to-pulse amplitude of the *Q*-switched pulse train showed a fluctuation of approximately less than 7.5%.

We report the whole evolutions of pulse width and pulse repetition rate in Fig. 10, from which one can see that at the threshold the pulse width is about 80.5 ns at a repetition rate of 5.8 kHz. With the increase of the absorbed power, the repetition rate almost linearly increased to the maximum value of 22.9 kHz, while the pulse width almost monotonously decreased to 18.2 ns despite exhibiting a small amount of saturation at the maximum. In this experiment, the maximum single-pulse

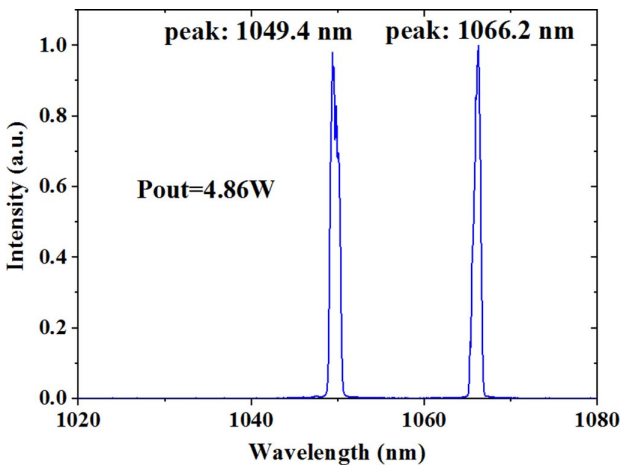

Fig. 7. Typical wavelength of dual-wavelength Nd:SRA laser after the insertion of the YAG etalon.

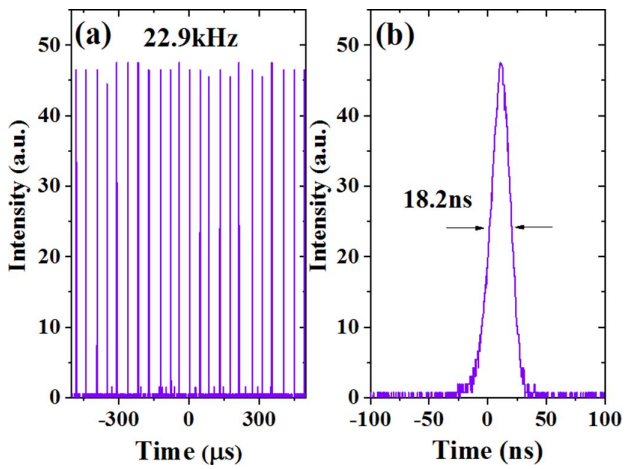

Fig. 9. (a) Typical pulse trains and (b) single-pulse profile of passively *Q*-switched Nd:SRA laser.

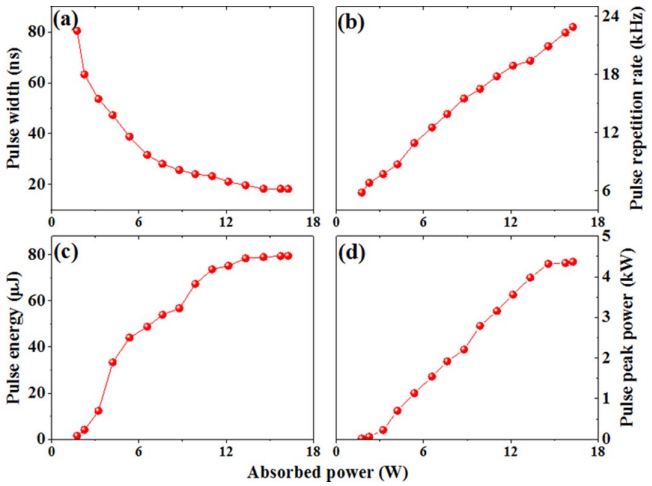

Fig. 10. Evolution of (a) pulse width, (b) pulse repetition rate, (c) pulse energy, and (d) pulse peak power versus absorbed power.

energy was achieved to be about 79.4 μJ, and the pulse peak power was about 4.3 kW. The saturation phenomenon is also reflected by the pulse energy and peak power. Anyway, these results are far better than the previous ones.

4. Conclusion

In summary, diode-end-pumped CW and passively *Q*-switched Nd:SRA lasers have been revisited, aiming at achieving high-performance operation. With respect to the CW operation, a maximum output power of 6.45 W is achieved at 1049 nm with a slope efficiency of about 41.6%. Moreover, a 1066 nm laser was also achieved by wavelength selection with a maximum output power of 4.15 W and a slope efficiency of about 27%. For passively *Q*-switched operation, the maximum average output power and the shortest pulse width reached 1.82 W and 18.2 ns, respectively. The single-pulse energy and pulse peak power were 79.4 μJ and 4.3 kW. On the one hand, the present results indicate that the Nd:SRA crystal is very promising for high-performance laser generation. On the other hand, by further optimizing the laser system, including improving the crystal quality, we expect that power scaling to more than 10 W with better efficiency could be realized in the future.

Acknowledgement

This work was partially supported by the National Natural Science Foundation of China (No. 61621001) and Qinglan Project of the Young and Middle-aged Academic Leader of Jiangsu College and University.

References

1. M. Rico, J. Liu, U. Griebner, V. Petrov, M. D. Serrano, F. Esteban-Betegón, C. Cascales, and C. Zaldo, "Tunable laser operation of ytterbium in disordered single crystals of Yb:NaGd$(WO_4)_2$," Opt. Express **12**, 5362 (2004).
2. H. H. Yu, H. J. Zhang, Z. P. Wang, J. Y. Wang, Y. Yu, Z. B. Shi, X. Y. Zhang, and M. H. Jiang, "High-power dual-wavelength laser with disordered Nd:CNGG crystals," Opt. Lett. **34**, 151 (2009).
3. Q. Wang, Z. Y. Wei, Y. D. Zhang, Z. G. Zhang, H. H. Yu, H. J. Zhang, J. Y. Wang, M. W. Gao, C. Q. Gao, and Z. L. Wang, "Tunable continuous-wave laser at quasi-three-level with a disordered Nd:LGS crystal," Opt. Lett. **36**, 1770 (2011).
4. X. F. Guan, Z. Y. Zhou, X. X. Huang, B. Xu, H. Xu, Z. Cai, X. D. Xu, and J. Xu, "Disordered Nd:$LuYSiO_5$ crystal lasers operating on the $^4F_{3/2}\rightarrow{}^4I_{11/2}$ and $^4F_{3/2}\rightarrow{}^4I_{13/2}$ transitions," Opt. Mater. **73**, 330 (2017).
5. G. Q. Xie, D. Y. Tang, W. D. Tan, H. Luo, H. J. Zhang, H. H. Yu, and J. Y. Wang, "Subpicosecond pulse generation from a Nd:CLNGG disordered crystal laser," Opt. Lett. **34**, 103 (2009).
6. Z. P. Qin, G. Q. Xie, J. Ma, W. Y. Ge, P. Yuan, L. J. Qian, L. B. Su, D. P. Jiang, F. K. Ma, Q. Zhang, Y. X. Cao, and J. Xu, "Generation of 103 fs mode-locked pulses by a gain linewidth-variable Nd,Y:CaF_2 disordered crystal," Opt. Lett. **39**, 1737 (2014).
7. J. Ma, Z. B. Pan, H. Q. Cai, H. H. Yu, H. J. Zhang, D. Y. Shen, and D. Y. Tang, "Sub-80 femtosecond pulses generation from a diode-pumped mode-locked Nd:$Ca_3La_2(BO_3)_4$ disordered crystal laser," Opt. Lett. **41**, 1384 (2016).
8. A. J. Lindop, C. Matthews, and D. W. Goodwin, "Refined structure of $Sr_{0.6}Al_2O_3$," Acta Crystallogr. B **31**, 2940 (1975).
9. M. Fechner, F. Reichert, N. O. Hansen, K. Petermann, and G. Huber, "Crystal growth, spectroscopy, and diode pumped laser performance of Pr, Mg:$SrAl_{12}O_{19}$," Appl. Phys. B **102**, 731 (2011).
10. F. Reichert, D. T. Marzahl, P. Metz, M. Fechner, N. O. Hansen, and G. Huber, "Efficient laser operation of Pr^{3+},Mg^{2+}:$SrAl_{12}O_{19}$," Opt. Lett. **37**, 4889 (2012).
11. T. Zhang, L. B. Zhou, J. Y. Zou, Y. K. Bu, B. Xu, X. D. Xu, and J. Xu, Laser performances of passively *Q*-switched Pr^{3+}-doped oxide lasers based on Pr^{3+}, Mg^{2+}:$SrAl_{12}O_{19}$ crystal and Co:ASL saturable absorber," Opt. Laser Technol. **139**, 106961 (2021).
12. M. F. Zhao, Z. M. Zhang, X. Y. Feng, M. Y. Zong, J. Liu, X. D. Xu, and H. Zhang, "High repetition rate passively *Q*-switched laser on Nd:SRA at 1049 nm with MXene $Ti_3C_2T_x$," Chin. Opt. Lett. **18**, 041401 (2020).
13. Y. X. Pan, B. Liu, J. Liu, Q. S. Song, J. Xu, D. Z. Li, P. Liu, J. Ma, X. D. Xu, H. Lin, J. Xu, and K. Lebbou, "Polarized spectral properties and laser operation of Nd:$SrAl_{12}O_{19}$ crystal," J. Lumin. **235**, 118034 (2021).
14. J. L. Lan, Y. Wang, X. X. Huang, Z. Lin, B. Xu, H. Xu, Z. Cai, X. D. Xu, and J. Xu, "Single- and dual-wavelength lasers of diode-pumped Nd:LuYAG mixed crystal on various $^4F_{3/2}\rightarrow{}^4I_{13/2}$ Stark-level transitions," J. Phys. D **49**, 305101 (2016).
15. Z. Lin, X. Huang, J. Lan, Y. Cheng, Y. Wang, B. Xu, H. Xu, and Z. Cai, "Efficient and compact diode-pumped Nd:YAG Lasers at 1073 and 1078 nm," IEEE Photon. J. **8**, 1500808 (2016).
16. B. Xu, Y. J. Cheng, Y. Wang, Y. Z. Huang, J. Peng, Z. Q. Luo, H. Xu, Z. Cai, J. Weng, and R. Moncorgé, "Passively *Q*-switched Nd:$YAlO_3$ nanosecond laser using MoS_2 as saturable absorber," Opt. Express **22**, 28934 (2014).
17. S. Han, Y. Zhou, Z. P. Wang, D. W. Hu, X. D. Xu, H. H. Yu, J. Xu, and X. G. Xu, "Graphene *Q*-switched 1.4 μm solid state laser," Laser Phys. Lett. **15**, 075801 (2018).
18. R. Dai, J. Chang, Y. Li, S. Shi, H. Li, Z. Yang, R. Ding, and M. Yang, "Performance enhancement of passively *Q*-switched Nd:YVO_4 laser using graphene–molybdenum disulphide heterojunction as a saturable absorber," Opt. Laser Technol. **117**, 265 (2019).
19. H. W. Zhang, J. Y. Peng, X. P. Yang, C. Ma, Q. Q. Zhao, G. L. Chen, X. Y. Su, D. C. Li, and Y. Zheng, "Passively *Q*-switched Nd:YVO_4 laser operating at 1.3 μm with a graphene oxide and ferroferric-oxide nanoparticle hybrid as a saturable absorber," Appl. Opt. **59**, 1741 (2020).